American Mineralogist, Volume 80, pages 907–915, 1995

$I\bar{1}$-$I2/c$ phase transition in alkaline-earth feldspars: Evidence from TEM observations of Sr-rich feldspars along the $CaAl_2Si_2O_8$-$SrAl_2Si_2O_8$ join

MARIO TRIBAUDINO, PIERA BENNA, EMILIANO BRUNO
Dipartimento di Scienze Mineralogiche e Petrologiche, Via Valperga Caluso 35, I-10125 Turin, Italy; and
Centro di Studi sulla Geodinamica delle Catene Collisionali (CNR), Via Accademia delle Scienze 5, I-10123 Turin, Italy

ABSTRACT

Domain textures related to the $I\bar{1}$-$I2/c$ displacive phase transition were observed by transmission electron microscopy (TEM) in synthetic samples from the Sr-rich region of the $CaAl_2Si_2O_8$-$SrAl_2Si_2O_8$ join. Albite and, more rarely, pericline transformation twins are formed in samples with preexisting polysynthetic Carlsbad twins; they also cut preexisting *b*-type antiphase domains. Tweed textures associated with albite twin lamellae were observed in triclinic samples and, more rarely, in monoclinic samples close to the transition point. Progressive annealing of a monoclinic disordered precursor was performed to follow the monoclinic-triclinic transition at room temperature. Triclinic and monoclinic phases coexisted close to the transition, whereas tweed textures, rarely present in monoclinic grains, were retained in the triclinic phase after longer annealing. In situ high-temperature TEM experiments performed on a grain with pericline twins showed that the pericline twins disappeared at T_c, but, during cooling, tweed textures appeared and then were replaced by albite twins at lower temperatures. The tweed textures are interpreted as originating from strain modulations induced by the displacive transition rather than modulation in Al-Si order, and they form close to the transition point as precursors of the albite and pericline twinning.

INTRODUCTION

Sr-rich feldspars from the $CaAl_2Si_2O_8$-$SrAl_2Si_2O_8$ (An-SrF) system, which are triclinic at room temperature, undergo a displacive $I\bar{1}$-$I2/c$ phase transition at higher temperature (Bruno and Gazzoni, 1968; Nager et al., 1970; Bambauer and Nager, 1981). The same transition is achieved at room temperature by increasing Sr content (Bambauer and Nager, 1981; McGuinn and Redfern, 1994a) (Fig. 1). In addition, it has been shown that at room temperature a monoclinic-triclinic $I2/c$-$I\bar{1}$ transition occurs in the Sr end-member feldspar at $P = 32$ kbar (McGuinn and Redfern, 1994b). This transition is analogous to the $C2/m$-$C\bar{1}$ displacive phase transition in disordered, topochemically monoclinic, alkali feldspars (Kroll et al., 1980). In alkali feldspars a connection between Al-Si order and the displacive phase transition was established by Laves (1960); subsequently, Salje (1985) and Salje et al. (1985b) recast these concepts within the framework of Landau theory, observing a coupling of the displacive transition with Al-Si order. Comparable coupling is suspected in alkaline-earth feldspars and might significantly affect the thermodynamic properties of pure anorthite and anorthite-bearing feldspars (McGuinn and Redfern, 1994a). In pure anorthite the displacive transition is expected to occur at a temperature well above the melting point ($T \approx 2770$ °C, Carpenter, 1992), whereas in Sr-rich feldspars it occurs in a temperature range that is easily accessible for experimental investigation (Fig. 1). Sr-rich feldspars evidently represent a useful model system for characterizing the thermodynamic behavior of anorthite-bearing feldspars.

Tribaudino et al. (1993) have shown that short isothermal annealing of gels with compositions in the Sr-rich field of the An-SrF join results in feldspars with a lower transition temperature, T_c, than that observed in well-ordered samples (Bambauer and Nager, 1981); the value of T_c increases with longer annealing times up to that observed in well-ordered samples. It was suggested that samples that have annealed for short times have disordered Al-Si configurations, and that longer annealing induces an increase in Al-Si order. There appear to be sufficient interactions between the Al-Si ordering and displacive processes to modify T_c. This proposed evolution of Al-Si order with annealing has recently been confirmed in Sr end-member feldspar by single-crystal X-ray study (Benna et al., 1995), and the possibility of biquadratic order-parameter coupling has been suggested also by McGuinn and Redfern (1994a), who examined the strain tensors of well-ordered samples synthesized along the An-SrF join.

One of the key features of any phase transition is the formation of a domain texture as a consequence of the symmetry reduction. The number of different domain types created in the low-symmetry form during a transition from a higher symmetry paraelastic phase can be predicted from the ratio of the number of symmetry elements in the point group of the high-symmetry phase

0003–004X/95/0910–0907$02.00

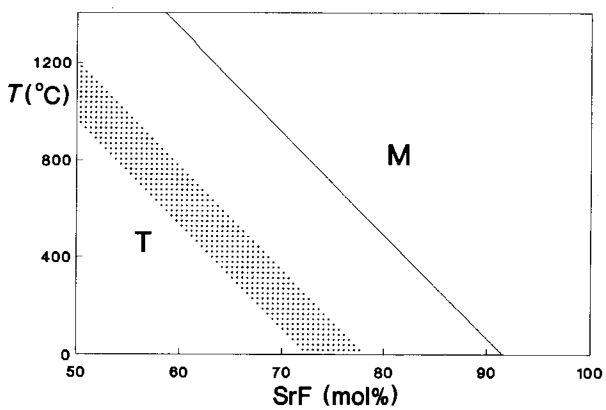

Fig. 1. T vs. composition diagram showing the monoclinic-triclinic boundary for Sr-rich feldspars. Continuous line: boundary for well-ordered Sr-rich feldspars (Bambauer and Nager, 1981; Tribaudino et al., 1993); shaded area: boundary between triclinic and monoclinic feldspars for samples after short annealing (T = 1480 °C, t = 2 h).

(four for $2/m$) to the number in the point group of the low-symmetry phase (two for $\bar{1}$) (Salje, 1990). Two transition-related twin domains are expected to form in triclinic samples for the $I2/c$-$I\bar{1}$ transition. Permissible orientations for the composition planes of these twins are parallel to (010) (albite twinning) and to **b** (pericline law) (Laves, 1952a, 1952b; Salje et al., 1985a), as observed in alkali feldspars that have undergone the $C2/m$-$C\bar{1}$ transition (Akizuki, 1983; Smith et al., 1987). Similar twins are expected to occur in triclinic Sr-rich feldspars; their distribution and interaction with other defects (e.g., antiphase domains associated with Al-Si ordering, preexisting growth twins) should provide new insights into the transformation behavior of alkaline-earth feldspars.

The purpose of this paper is to present the results of a TEM investigation of microstructures in experimental samples from the Sr-rich region of the $CaAl_2Si_2O_8$-$SrAl_2Si_2O_8$ join (between $SrF_{60}An_{40}$ and $SrF_{80}An_{20}$). Observations at room temperature and in situ at high temperature were performed.

Experimental methods

TEM investigations were performed on synthetic feldspars with compositions $SrF_{60}An_{40}$, $SrF_{70}An_{30}$, $SrF_{75}An_{25}$, and $SrF_{80}An_{20}$. The starting materials were gels prepared according to the method of Biggar and O'Hara (1969). Syntheses were conducted in an electric furnace (SiC resistance, Pt-PtRh 10% thermocouple) using unsealed Pt tubes and with subsequent quenching in air. The synthesis products were first examined by X-ray powder diffraction (Guinier camera, Cu$K\alpha$ radiation, λ = 1.54178 Å) and then by electron microscopy. TEM observations were performed on crushed grains deposited on a holey carbon film using a Philips CM-12 electron microscope operating at 120 kV and equipped with a double-tilt goniometer stage. Thermal treatments, TEM results, and unit-cell parameters are reported in Table 1. In situ high-temperature TEM observations were performed with a Gatan 652 double-tilt heating stage.

Domain structures

Carlsbad growth twinning

Bright- and dark-field images commonly display polysynthetic twinning that can be interpreted according to the Carlsbad law in monoclinic samples; in the triclinic samples the Carlsbad twins are associated with albite twins (Fig. 2). A high-resolution image of one twin is shown in Figure 3. Carlsbad twins are known to occur in $I2/c$ Sr-rich feldspar from single-crystal X-ray diffraction studies by Bruno and Gazzoni (1970); Töpel-Schadt et al. (1978) showed by TEM that they can be polysynthetic. The Carlsbad twinning frequency is higher in samples annealed for short periods. SAD patterns from these samples show strong streaking and an elongation of the diffraction spots parallel to **b***; the width of the lamellae is <100 Å. In samples subjected to longer thermal treatments, the twins are still polysynthetic, but their width and spacing increase significantly. The width of individual twins is rather variable, ranging from <50 to 2000–3000 Å. By way of comparison, Carlsbad twins seem to be relatively rare and never polysynthetic in anorthite samples prepared under similar experimental conditions (Kroll and Müller, 1980; Carpenter, 1991). There is, however, a close similarity in frequency between the polysynthetic Carlsbad twinning in Sr-rich feldspars and the polysynthetic albite twinning in anorthite after short devitrification from glass starting materials (Kroll and Müller, 1980; Carpenter, 1991). Both can be interpreted as growth twins, which occur with higher periodicity after short heat treatment. Albite growth twins may be preferred on the An-rich side of the join, but the frequency of Carlsbad twins increases dramatically in Sr-rich feldspars that, under our experimental conditions, grow with monoclinic symmetry (Bambauer and Nager, 1981; Tribaudino et al., 1993) for which the formation of albite twinning is symmetry forbidden.

Albite transformation twinning

In triclinic samples, albite twins are always associated with Carlsbad twins. Albite lamellae are more regular, varying from 300 to 1000 Å in width (Fig. 2), although their frequency is difficult to evaluate because of the presence of polysynthetic Carlsbad twinning with the same (010) composition plane. Triclinic symmetry is easily detected in SAD patterns down [100] or [001] axes by the splitting of reflections parallel to **b*** from albite twinning. In Sr-rich samples, which are monoclinic at the annealing temperature, albite twinning originates only during cooling as a consequence of the loss of the mirror plane because of the $I2/c$-$I\bar{1}$ transition. The result is a superposition of Carlsbad (growth) and albite (transformation) twins at room temperature.

TABLE 1. Thermal treatments and experimental results

SrF/An	T (°C)	t (h)	r.t.	APD (Å)	TD	Sym.	r.n.	a (Å)	b (Å)	c (Å)	α (°)	β (°)	γ (°)	V (Å³)
60/40	1500	0.033	a,(b)	n.m.	Ab	M/T	14	8.347(5)	12.955(8)	14.254(12)	90	115.12(11)	90	1395.6
60/40	1480	2	a,b	300	Ab	T	18	8.318(8)	12.945(9)	14.232(11)	91.40(10)	115.58(11)	90.90(9)	1381.2
60/40	1490	15	a,b	500	Ab,t	T	23	8.322(5)	12.929(4)	14.238(7)	91.80(4)	115.46(7)	90.96(3)	1381.7
60/40	1350	456	a,b	n.m.	Ab	T	27	8.313(2)	12.934(2)	14.238(3)	91.82(2)	115.61(3)	91.06(1)	1378.9
60/40	1350	456+												
	1520	2	a,b	850	Ab,(P),t	T	27	8.321(2)	12.930(3)	14.238(3)	91.81(2)	115.61(4)	91.08(2)	1379.9
70/30	1350	0.025	a,(b)	n.m.		M	12	8.360(7)	12.953(5)	14.255(11)	90	115.18(13)	90	1396.8
70/30	1350	0.10	a,(b)	40		M	13	8.363(3)	12.978(6)	14.258(9)	90	115.19(8)	90	1400.3
70/30	1350	0.25	a,(b)	n.m.		M	14	8.360(4)	12.954(6)	14.255(11)	90	115.29(9)	90	1395.7
70/30	1350	0.66	a,(b)	n.m.	(Ab)	M	14	8.359(4)	12.974(8)	14.258(12)	90	115.22(10)	90	1399.2
70/30	1350	1.5	a,b	n.m.	Ab	M/T	14	8.358(4)	12.965(5)	14.253(9)	90	115.32(7)	90	1396.1
70/30	1350	14	a,b	350	Ab,P	T	21	8.349(5)	12.965(6)	14.251(8)	91.06(8)	115.45(9)	90.68(6)	1392.3
70/30	1350	136	a,b	560	Ab,t	T	25	8.345(2)	12.954(2)	14.255(4)	91.33(3)	115.54(3)	90.86(2)	1389.6
70/30	1350	1073	a,b	2000	Ab	T	21	8.347(2)	12.958(3)	14.253(4)	91.43(3)	115.54(4)	90.89(3)	1389.8
70/30	1250	1090	a,b	1400	Ab	T	24	8.338(2)	12.956(3)	14.253(4)	91.34(3)	115.52(4)	90.90(2)	1388.5
70/30	1480	2	a,b	300	Ab,t	T	18	8.337(8)	12.952(5)	14.237(6)	91.11(6)	115.56(8)	90.68(7)	1386.3
70/30	1150	89	a,b	240		M	14	8.366(4)	12.979(6)	14.257(10)	90	115.27(9)	90	1399.9
70/30	1190	452	a,b	250	t	M/T	16	8.360(6)	12.973(9)	14.256(13)	90.25(13)	115.39(11)	90.22(9)	1396.7
75/25	1480	2	a,b	300	Ab,t	M/T	16	8.371(7)	12.962(7)	14.247(9)	90	115.11(9)	90	1397.7
75/25	1480	17	a,b	500	Ab	T	20	8.338(7)	12.959(5)	14.249(7)	91.06(5)	115.53(9)	90.79(6)	1388.7
75/25	1450	542	a,b	8000	Ab,t	T	24	8.359(5)	12.950(5)	14.259(7)	91.19(5)	115.50(9)	90.84(4)	1392.5
80/20	1350	456	a,b	n.m.	Ab	M/T	17	8.360(7)	12.964(9)	14.261(14)	90.67(13)	115.41(13)	90.32(8)	1395.9
80/20	1350	222+												
	1450	63	a,b	1000	Ab,(P),t	T	24	8.359(5)	12.938(6)	14.255(6)	90.77(4)	115.38(8)	90.65(4)	1392.5
80/20	1350	456+												
	1530	2	a,b	2000	Ab,(P),t	T	24	8.350(5)	12.966(4)	14.261(6)	90.72(4)	115.41(8)	90.66(4)	1394.4

Note: compositions (in mole percent), experimental conditions, reflection type present in SAD patterns (r.t.), antiphase domain size (APD), $I\bar{1}$-$I2/c$ transition related domains (TD), symmetry (Sym), number of reflections used to refine lattice parameters (r.n.) and unit-cell parameters. Ab: albite transformation twinning; P: pericline twinning; (P): pericline-like lamellae without diffraction evidence; t: tweed texture; n.m.: not measured; M: monoclinic; T: triclinic; M/T: monoclinic and triclinic reflections coexisting in powder spectra.

Pericline twinning

In some grains a few lamellae that cross the albite twin walls almost at right angles were observed (Fig. 4). Pericline twins are nearly perpendicular to (010), but diffraction evidence confirming their identification is difficult to obtain because of their scarcity (Fitz Gerald and McLaren, 1982). Conclusive diffraction evidence was observed only in a $SrF_{70}An_{30}$ sample (T = 1350 °C, t = 14 h), in an area where only pericline twinning was present (Fig. 5a). Note from Figure 5a that the pericline twins taper to the edge of a Carlsbad twin (top of the photo). Similar needle-like junctions were previously observed between transformation-related domains (Salje, 1990).

Tweed microstructures

A tweed microstructure was observed, more commonly than pericline twinning, preferentially oriented normal to (010) and, to a lesser extent, parallel to (010). The microstructure is generally associated with albite lamellae and gives characteristic crossed streaks through many reflections in SAD patterns. This tweed texture was observed in triclinic samples and in monoclinic samples close to the transition (Figs. 4 and 6).

Similar textures have been observed in orthoclase (McConnell, 1965), cordierite (Putnis et al., 1987), triclinic anorthoclase (Smith et al., 1987), and kinetically disordered albite (Wruck et al., 1991). At X-ray and SAD pattern scales, samples exhibiting the tweed pattern have the average structure and symmetry of the high-symmetry form in each case, but locally, within the modulation, the structure must be more like that of the low-symmetry form. Modulated textures of this type are usually interpreted as being closely associated with some phase transition. In this work tweed textures observed within triclinic grains are associated with 2000 Å wide albite lamellae ascribed to the displacive transition.

The *b*-type antiphase domains

Microstructures attributed to *b*-type antiphase domains were observed in samples within the composition range $SrF_{60}An_{40}$–$SrF_{80}An_{20}$ (Fig. 7). These domains are connected with ordering of Al-Si tetrahedral cations, which induces a zone-boundary transition from the C (7 Å) lattice for disordered feldspars to the I (14 Å) lattice for ordered feldspars with Al:Si = 1:1. In triclinic crystals the symmetry change is from $C\bar{1}$ to $I\bar{1}$ and in monoclinic crystals from $C2/m$ to $I2/c$. Al-Si ordering requires the breaking of strong bonds within the tetrahedra and is extremely sluggish compared with the monoclinic-triclinic zone-center displacive transition.

The dimensions of the domains are given in Table 1. The domains are considered to develop within a $C2/m$ parent structure with a metastable disordered Al-Si configuration. Their development in Sr end-member feldspar is related to the onset of Al-Si ordering (Benna et al., 1995) without the initial appearance of e reflections as observed in anorthite (Carpenter, 1991). The transition from the C to the I lattice occurs after short annealing

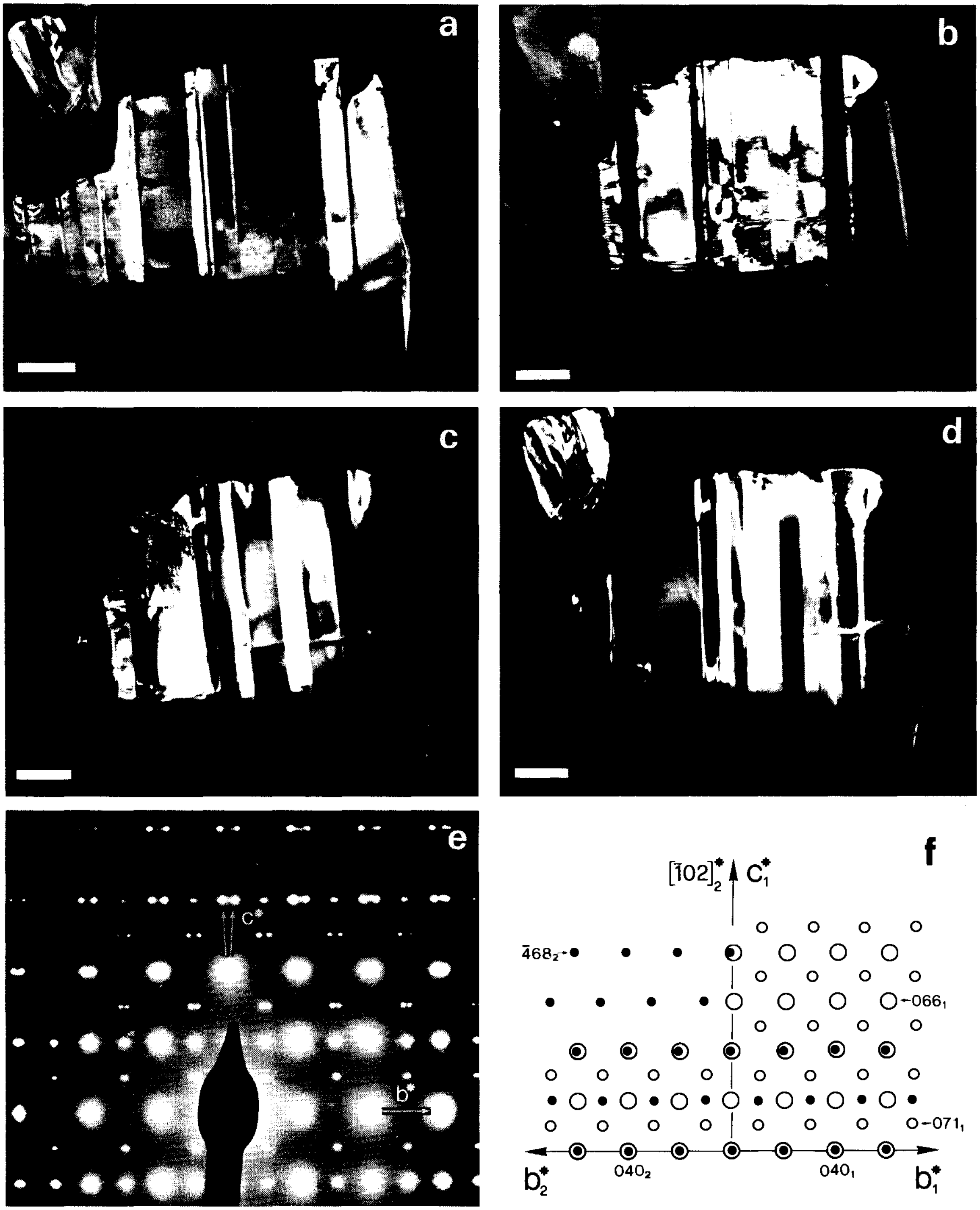

Fig. 2. $SrF_{80}An_{20}$ sample (T = 1350 °C, t = 456 h + T = 1530 °C, t = 2 h). Dark-field images of albite and Carlsbad twins; scale bar: 0.2 μm. (**a** and **b**) Carlsbad-twinned individuals, **g** = $\overline{15}2_2$ and **g** = 062_1. In **b**, composition planes normal to (010) and tweed textures are observed. (**c** and **d**) Albite twins within the Carlsbad individual visible in **b**, **g** = 006_{1a} and **g** = 006_{1b}. (**e**) SAD pattern from the same grain. Note streaking parallel to **b***. Albite twinning is indicated by arrows. This **b***-**c*** plane is superimposed by the **b***-[$\bar{1}$02]* plane of the other Carlsbad-twinned individual. (**f**) Schematic representation of Carlsbad twin shown in **e**. Open circles: individual 1 ($\mathbf{b}^*_1$-$\mathbf{c}^*_1$ plane); solid circles: individual 2 ($\mathbf{b}^*_2$-$[\bar{1}02]^*_2$ plane). The spots of individual 1 are split further according to the albite law.

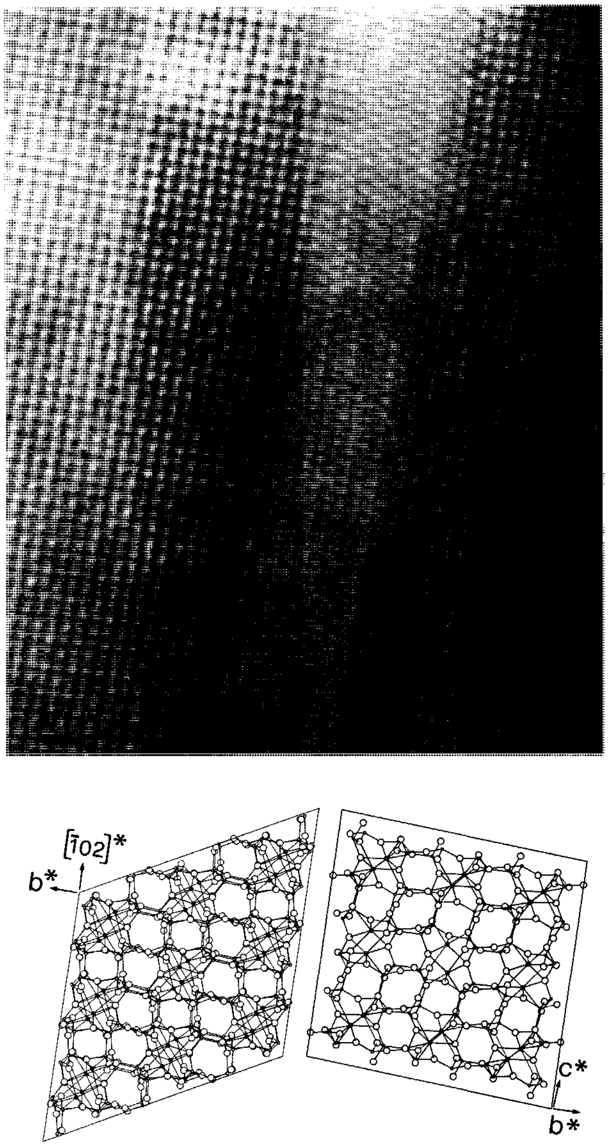

Fig. 3. Same sample as in Fig. 2. High-resolution image of Carlsbad twin along $[100]_1$ and $[201]_2$ directions. Note the absence of strain at the interface because of the very low structural misfit along the composition plane. Arrows (bottom of the photo) show the projection of the anorthite structure along the same directions.

times: for the composition $SrF_{70}An_{30}$ (at $T = 1350$ °C), b reflections were observed in only a few grains after annealing for periods of 0.025 and 0.25 h; in other grains, b reflections are faint. For samples annealed for longer than 0.25 h and shorter than 1 h, b reflections are always faint but not diffuse (Table 1). The largest domain sizes observed were ~8000 Å; size increases with annealing, as has been observed in pure anorthite (Kroll and Müller, 1980; Carpenter, 1991) and Sr end-member feldspar (Benna et al., 1995).

No c ($h + k = 2n$, $l = 2n + 1$) or d ($h + k = 2n + 1$, $l = 2n$) reflections were observed. These would be indicative of the 14 Å P lattice found in pure anorthite.

Fig. 4. Same sample as in Fig. 2. Tweed texture. Large albite twins demonstrate the triclinic symmetry of the grain; a pericline lamella is shown by the arrow. Dark field, **g** = 062; scale bar: 0.1 μm.

Textural evolution at room and high temperature

On the basis of these results, the monoclinic-triclinic $I2/c$-$I\bar{1}$ phase transition can be investigated (1) at room temperature, by changing the annealing time at constant composition and annealing temperature; or (2) by in situ heating of a triclinic Sr-rich sample.

Effect of annealing history

It was shown previously (Bambauer and Nager, 1981; Tribaudino et al., 1993) that samples with compositions between $SrF_{60}An_{40}$ and $SrF_{91}An_9$ annealed at high temperatures for short times are monoclinic when observed at room temperature but become triclinic when annealed for longer times. At first, monoclinic symmetry and relatively sharp powder patterns are observed by X-ray powder diffraction. The reflections become more diffuse, at least those becoming equivalent in a monoclinic system, as the transition is approached. The transition is marked by the coexistence of a "monoclinic" single reflection and two "triclinic" broad split reflections. Subsequent annealing induces further sharpening of reflections and increased triclinicity. It must be stressed that the

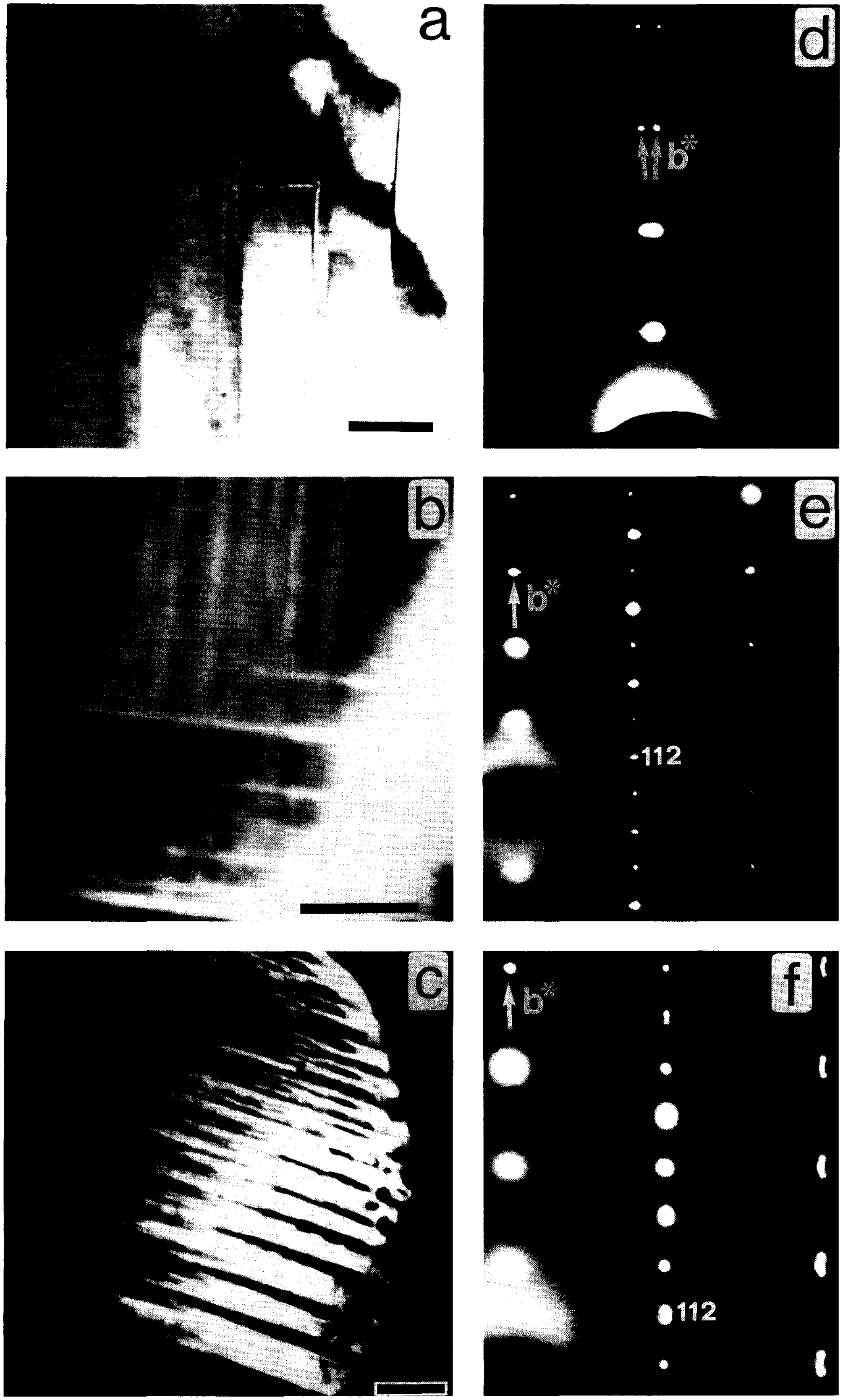
a
b
c
d
b*
e
b*
112
f
b*
112

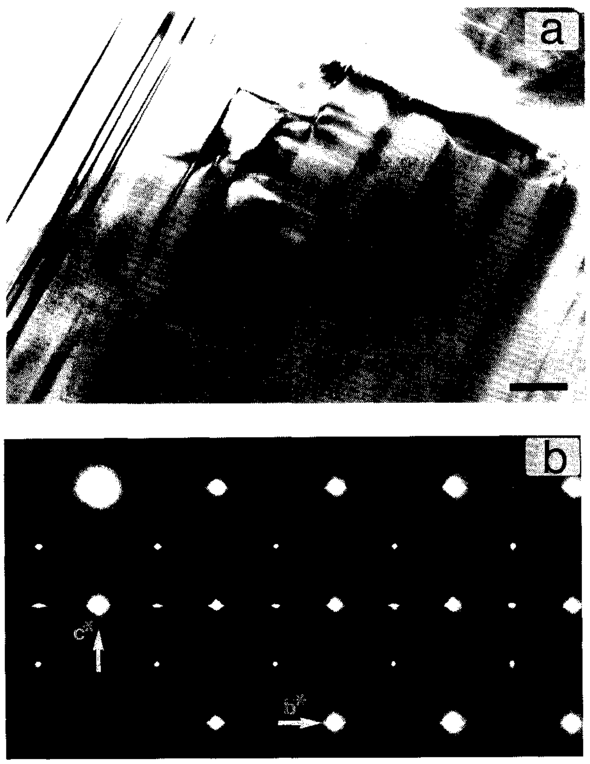

Fig. 6. $SrF_{75}An_{25}$ sample (T = 1480 °C, t = 2 h). (**a**) Tweed texture. A few thin Carlsbad twins are present on the left. Bright field, scale bar: 0.1 μm. (**b**) Related diffraction pattern. Note diffuse cross streaking in SAD pattern. The grain is probably monoclinic, as suggested by the absence of albite twinning.

Fig. 7. Same sample as in Fig. 2. The b-type antiphase domains. Albite twinning intersects the b antiphase domains. Arrows indicate antiphase domain boundaries displaced by albite twinning. The small misfit on the contact plane may be related to the low values of the 2ϕ obliqueness (ϕ = **b** $\wedge$ **b***) for these compositions. Dark field, **g** = $0\bar{3}5$; scale bar: 0.2 μm.

equilibrium structure of all these samples at room temperature has triclinic symmetry (Bambauer and Nager, 1981) and that the monoclinic crystals are only metastable.

Room temperature TEM and X-ray observations on monoclinic samples reveal a microstructure consisting of polysynthetic Carlsbad lamellae with a periodicity smaller than 100 Å and no evidence of tweed. After longer annealing, a monoclinic single reflection coexists (in X-ray powder patterns) with two triclinic broad split reflections. Electron diffraction patterns and dark- and bright-field images of several grains of one of these samples ($SrF_{75}An_{25}$, T = 1480 °C, t = 2 h) show that grains of different symmetry coexist within the same sample. This sample contains: (1) triclinic albite-twinned grains with sharp SAD patterns and few Carlsbad twins; individual twins ~50 Å are interspersed with intervals >500 Å free of albite or Carlsbad twin boundaries; (2) grains showing monoclinic symmetry; and (3) grains, with SAD patterns that are heavily streaked along **b*** because of polysynthetic Carlsbad twinning, that show an intermediate degree of triclinicity, as shown by the splitting of albite twin-related reflections. Each texture is uniform over grains up to a few hundred angstroms in size, and tweed textures are very rare. The coexistence of triclinic and monoclinic reflections in X-ray diffraction patterns thus indicates heterogeneities in structural state at least over this length scale.

Further annealing results in the appearance of transition-related features such as albite twinning and, rarely, pericline twinning. The Carlsbad and albite twin frequencies decrease with annealing. Significant changes in unit-cell parameters are also observed, mostly in α and γ (Table 1), up to the values obtained by Bambauer and Nager (1981), Tribaudino et al. (1993), and McGuinn and Redfern (1994a) for well-ordered samples.

One interpretation of the heterogeneity found in the $SrF_{75}An_{25}$ sample (T = 1480 °C, t = 2 h) could be heterogeneity in the degree of Al-Si order together with coupling between the displacive and the order-disorder transitions. Al-Si ordering could affect the transition temperature, consistent with the experimental observations of samples

←

Fig. 5. In situ heating cycle of $SrF_{70}An_{30}$ sample (T = 1350 °C, t = 14 h). Scale bars: 0.1 μm. (**a**) Room temperature, before heating. Pericline twinning associated with thin (horizontal) Carlsbad lamellae. The sample was oriented normal to the calculated rhombic section. Bright field. (**b**) At $T > T_c$ ($T \approx 500$ °C, nominal furnace temperature), after the disappearance of pericline twinning. The image was taken during cooling. A tweed texture with predominant pericline orientation is observed. Horizontal Carlsbad lamellae are present (bottom of the photo). Dark field, **g** = $1\bar{3}2$. (**c**) At room T at the end of the cooling. Pericline twins have been replaced by albite twinning. Dark field, **g** = $1\bar{3}2$. (**d**, **e**, and **f**) Corresponding SAD patterns. In **e** the diffraction pattern shows an elongation of the spots along and parallel to **b***, probably because of incipient pericline and albite twinning.

with different annealing histories (Tribaudino et al., 1993). Grains with different degrees of Al-Si order might be considered as separate blocks that attain the transition at different temperatures. Differences in the degree of order at a scale of a few thousand angstroms could originate from heterogeneity in Al-Si order within the gel starting material and disappear only after longer heating and attainment of equilibrium.

The broadening of reflections that are nonequivalent under triclinic symmetry and the coexistence of monoclinic and triclinic phases have also been observed by in situ powder diffraction measurements at high temperature (Tribaudino et al., 1993) for samples with intermediate annealing times. From Figure 1 it appears that at room temperature the $SrF_{75}An_{25}$ sample (T = 1480 °C, t = 2 h) would be within the coexistence range, and that nucleation and growth of triclinic grains would not be completed.

The heterogeneity in structural state found in the $SrF_{75}An_{25}$ sample could be connected with a possible compositional heterogeneity, i.e., locally variable Ca-Sr ratios, at the required length scale, since even small changes in composition significantly affect the transition temperature (Fig. 1). However, X-ray powder lines are relatively sharp both before and after the transition, whereas a compositional heterogeneity should cause a significant broadening in diffraction lines.

Recently, Harrison and Salje (1994) observed a broadening in peak widths close to the monoclinic-triclinic transition in hypersolvus anorthoclase that has been suggested to depend on the grain size of the sample. Their analysis considered surface relaxation, which might have some influence on the X-ray powder evidence of the present work. Further experimental data are required to clarify the relative influence of the coupling between the displacive and the order-disorder transitions and of surface relaxation.

In situ behavior at high temperatures

High-temperature in situ TEM analysis was performed to follow the evolution of albite and pericline twins in grains containing only one type of twinning, at least in the area of observation. Albite twinning was examined in the $SrF_{75}An_{25}$ sample (T = 1480 °C, t = 2 h), and pericline twinning was examined in a $SrF_{70}An_{30}$ sample (T = 1350 °C, t = 14 h). In both cases, SAD patterns show that heating up to the transition temperature induces a decrease in the twin-related splittings. Bright- and dark-field imaging does not reveal a change in the position of the twin boundaries with heating, but differences arise after the sample is heated into the high-symmetry field. In the grain with initial pericline twins (Fig. 5a), the lamellae disappeared at the transition point and did not reappear on cooling. Instead a tweed texture developed on cooling, with a predominant pericline orientation (Fig. 5b). No diffraction evidence for twinning was present apart from elongation of the spots along and perpendicular to **b***. Further cooling induced the formation of albite twinning that grew at the expense of the tweed texture (Fig. 5c). Growth of albite twinning is rather fast (about 0.1 μm/s). The tweed texture formed again during subsequent heating, at the expense of albite twinning, and disappeared at higher temperatures. Repeated cooling yielded tweed textures at higher temperatures and the growth of albite twins at lower temperatures, but at no stage did the initial pericline twinning reappear. Tweed textures seem to be a pretransition feature in this grain. *S*-shaped boundaries are observed as remnants of formerly intersecting albite and pericline twin walls (Fig. 5c). Similar features have been observed in superconducting $YBa_2Ca_3O_7$ (Salje, 1990).

In an in situ investigation of the monoclinic-triclinic transition in anorthoclase, Smith et al. (1987) observed that, in areas where both types of twinning were present, albite twinning is favored at temperatures further from the transition point, whereas pericline twinning is more stable close to the transition. In the $SrF_{70}An_{30}$ sample, we found that tweed textures develop close to the transition, with pericline-like modulations predominant. Extremely sluggish Al-Si ordering in alkaline-earth feldspars prevents a change in Al-Si order during in situ heating experiments. The tweed textures are therefore interpreted as strain modulations induced by the displacive transition.

In the albite-twinned grain, twin boundaries disappeared at the transition temperature and formed again during cooling. No tweed textures were observed at any stage of the heating and cooling cycle. This suggests that tweed textures do not always form across the transition. Instead nucleation of albite twins apparently occurs with no intermediate state.

There are slight differences between tweed textures observed during the in situ experiments across the transition and those observed at room temperature in samples well within the triclinic stability field. In the former, the pericline-like orientation predominates, whereas in the latter it does not. The contrast is sharper in the first case and fainter in the second, but in neither case were interfaces present between the boundaries. Given that the tweed microstructure is, in general, a mechanism for relieving spontaneous strain (Nord, 1994) without forming twin boundaries, it is not surprising that different thin flakes might behave differently since they probably have different strain fields according to their exact size and shape.

It should be noted that at room temperature in modulated triclinic samples, twin boundaries cut sharply across the modulations, suggesting that the albite twinning developed after the modulations formed. No evidence was found of discrete albite twinning developing within the tweed texture.

Acknowledgments

Reviews from M.A. Carpenter and S. Ghose greatly improved the manuscript. This work was supported by Ministero della Ricerca Scientifica e Tecnologica and CNR, Rome.

References cited

Akizuki, M. (1983) An electron microscopic study of anorthoclase spherulites. Lithos, 16, 249–254.

Bambauer, H.U., and Nager, H.E. (1981) Gitterkonstanten und displazive Transformation synthetischer Erdalkalifeldspäte: I. System $Ca[Al_2Si_2O_8]$-$Sr[Al_2Si_2O_8]$-$Ba[Al_2Si_2O_8]$. Neues Jahrbuch für Mineralogie Abhandlungen, 141, 225–239.

Benna, P., Tribaudino, M., and Bruno, E. (1995) Al-Si ordering in Sr-feldspar $SrAl_2Si_2O_8$: IR, TEM and single crystal XRD evidences. Physics and Chemistry of Minerals, in press.

Biggar, G.M., and O'Hara, M.J. (1969) A comparison of gel and glass starting materials for phase equilibrium studies. Mineralogical Magazine, 36, 198–205.

Bruno, E., and Gazzoni, G. (1968) Feldspati sintetici della serie $CaAl_2Si_2O_8$-$SrAl_2Si_2O_8$. Atti dell'Accademia delle Scienze di Torino, 102, 881–893.

——— (1970) Single-crystal X-ray investigation on strontium feldspar. Zeitschrift für Kristallographie, 132, 327–331.

Carpenter, M.A. (1991) Mechanisms and kinetics of Al-Si ordering in anorthite: I. Incommensurate structure and domain coarsening. American Mineralogist, 76, 1110–1119.

——— (1992) Equilibrium thermodynamics of Al/Si ordering in anorthite. Physics and Chemistry of Minerals, 19, 1–24.

Fitz Gerald, J.D., and McLaren, A.C. (1982) The microstructures of microcline from some granitic rocks and pegmatites. Contributions to Mineralogy and Petrology, 80, 219–229.

Harrison, R.J., and Salje, E. (1994) X-ray diffraction study of the displacive phase transition in anorthoclase, grain-size effects and surface relaxations. Physics and Chemistry of Minerals, 21, 325–329.

Kroll, H., and Müller, W.F. (1980) X-ray and electron-optical investigation of synthetic high-temperature plagioclases. Physics and Chemistry of Minerals, 5, 255–277.

Kroll, H., Bambauer, H.U., and Schirmer, U. (1980) The high albite-monalbite and analbite-monalbite transitions. American Mineralogist, 65, 1192–1211.

Laves, F. (1952a) Phase relations of the alkali feldspars: I. Introductory remarks. Journal of Geology, 60, 436–450.

——— (1952b) The phase relations of the alkali feldspars: II. Journal of Geology, 60, 549–574.

——— (1960) Al/Si-Verteilungen, Phasen-Transformationen und Namen der Alkalifeldspäte. Zeitschrift für Kristallographie, 113, 265–296.

McConnell, J.D.C. (1965) Electron optical study of effects associated with the partial inversion of a silicate phase. Philosophical Magazine, 11, 1289–1301.

McGuinn, M.D., and Redfern, S.A.T. (1994a) Ferroelastic phase transition along the join $CaAl_2Si_2O_8$-$SrAl_2Si_2O_8$. American Mineralogist, 79, 24–30.

——— (1994b) Ferroelastic phase transition in $SrAl_2Si_2O_8$ feldspar at elevated pressure. Mineralogical Magazine, 58, 21–26.

Nager, H.E., Bambauer, H.U., and Hoffmann, W. (1970) Polymorphie in der Mischreihe (Ca,Sr) $[Al_2Si_2O_8]$. Naturwissenschaften, 57, 86–87.

Nord, G.L., Jr. (1994) Transformation induced twin boundaries in minerals. Phase Transitions, 48, 107–134.

Putnis, A., Salje, E., Redfern, S.A.T., Fyfe, C.A., and Strobl, H. (1987) Structural states of Mg-cordierite: I. Order parameters from synchrotron X-ray and NMR data. Physics and Chemistry of Minerals, 14, 446–454.

Salje, E. (1985) Thermodynamics of sodium feldspar: I. Order parameter treatment and strain induced coupling effects. Physics and Chemistry of Minerals, 12, 93–98.

——— (1990) Phase transitions in ferroelastic and co-elastic crystals, 366 p. Cambridge University Press, Cambridge, U.K.

Salje, E., Kuscholke, B., and Wruck, B. (1985a) Domain wall formation in minerals: I. Theory of twin boundary shapes in Na-feldspar. Physics and Chemistry of Minerals, 12, 132–140.

Salje, E., Kuscholke, B., Wruck, B., and Kroll, H. (1985b) Thermodynamics of sodium feldspar: II. Experimental results and numerical calculations. Physics and Chemistry of Minerals, 12, 99–107.

Smith, K.L., McLaren, A.C., and O'Donnell, R.G. (1987) Optical and electron microscope investigation of temperature dependent microstructures in anorthoclase. Canadian Journal of Earth Science, 24, 528–543.

Töpel-Schadt, J., Müller, W.F., and Pentinghaus, H. (1978) Transmission electron microscopy of $SrAl_2Si_2O_8$: Feldspar and hexacelsian polymorphs. Journal of Material Science, 13, 1809–1816.

Tribaudino, M., Benna, P., and Bruno, E. (1993) $I\bar{1}$-$I2/c$ phase transition in alkaline-earth feldspars along the $CaAl_2Si_2O_8$-$SrAl_2Si_2O_8$ join: Thermodynamic behaviour. Physics and Chemistry of Minerals, 20, 221–227.

Wruck, B., Salje, E., and Graeme-Barbcr, A. (1991) Kinetic rate laws derived from order parameter theory: IV. Kinetics of Al-Si disordering in Na-feldspars. Physics and Chemistry of Minerals, 17, 700–710.

Manuscript received November 4, 1994
Manuscript accepted May 8, 1995